The Synthesized Reduced Graphene Oxide Enhanced the Capacitive Behavior of Activated Carbon/PVA as Potential Electrode Materials

Nurhafizah Md Disa [1,2]*, Khor Shi Yuan [2], Khye Lee Tan [2], and Soga Tetsuo [3]

[1] *Nano-Optoelectronic Research and Technology Laboratory, Universiti Sains Malaysia, 11800 Minden, Penang, Malaysia*

[2] *School of Physics, Universiti Sains Malaysia, 11800 Minden Penang, Malaysia*

[3] *Department of Frontier Materials, Nagoya Institute of Technology, Gokiso-cho, Showa-ku, Nagoya, Japan*

ARTICLE INFO

ABSTRACT

In this work, activated carbon (AC) derived from biomass wastes was implemented as electrode materials in supercapacitor application. This study has adopted rubber seed shell (RSS) wastes to derive AC via pyrolysis process. Meanwhile, reduced graphene oxide (rGO) was used as an additive material in order to study the effect of the rGO in capacitive behavior. The synthesized rGO was successfully produced through the electrochemical exfoliation method then further chemically reduced the solution using hydrazine hydrate. Four different electrodes were fabricated using a spin coating method to investigate the effect of added rGO to the capacitive behavior. One sample of AC/polyvinyl alcohol (PVA) as reference was prepared with ratio 2:8. Meanwhile, the three samples were prepared with different volumes of rGO. A series of techniques to characterize the morphological and structural properties of the samples have been carried out using field emission scanning electron microscopy (FESEM), energy dispersive x-ray (EDX), atomic force microscopy (AFM), and Brunauer-Emmett-Teller (BET) surface analysis. Based on the cyclic measurements, $AC/PVA/rGO_2$ showed the lowest resistivity which was 3.74 and consequently enhanced at least 10 orders in capacitive performance as compared to bare AC/PVA. Therefore, the capability of small amount rGO in enhancing the capacitive behavior paves the way for versatile practical applications in the electronic field.

INTRODUCTION

Recently, the supercapacitor market is rapidly growing, particularly in the automotive sector. There has been an increasingly wider use of supercapacitors technology, replacing batteries in some cases, and in others complementing their performance [1-3]. Activated carbon (AC) is the most widely used as electrode material in the fabrication of a supercapacitor due to its large surface area, microporous structure, and good electrical as well as chemical properties. Basically,

AC is derived from coal. These coal-based AC has undergone a steam activation process, and create millions of small, low-volume pores on the surface of the carbon, thereby increasing its total surface area. However, coal-based AC is expensive, unsustainable and may negatively impact the environment. Thus, many researchers have found alternative materials that can be replace with coal-based AC, such as bamboo, coconut shell, oil palm shell, cotton, pine nut shell, as well as other nut shell waste [2-3]. In this study, AC

* Corresponding Author Email: mdnurhafizah@usm.my

derived from rubber seed shell (RSS) is used as a conductive material to be utilized as an electrode in a supercapacitor.

Numerous researchers have found that there is a discrepancy in the relationship between specific capacitance and specific surface area (SSA) of AC. All the pores are not effective and suitable for the electrolyte during the formation of electric double layer, so small capacitance can be obtained despite having a high SSA. Suitable pore size distribution has greater influence on the capacitance than the SSA. Using a suitable structure of porous electrode material that matches with the size of the electrolyte ions can improve the electrochemical characteristics of the supercapacitors [4-6]. Although, excessive activation results in large pore volume, it has drawbacks such as low conductivity and material density, resulting in low energy density and loss of power capability [5]. Thus, a conductive material, reduced graphene oxide (rGO), was used as an additive to overcome these shortcomings. Moreover, rGO was used due to its outstanding characteristics in terms of improved electrical conductivity, high surface area, and low-cost. This makes rGO a promising material to be implemented in electronic devices.

In this work, the synthesis of AC from rubber seed shell (RSS) was performed via pyrolysis process. The scope of this study was to understand the effect of various volumes of rGO (1 wt%, 2 wt% and 3 wt%) in the electrodes to the capacitance performance of the supercapacitors. Thus, the best configuration of electrode materials for supercapacitor application was investigated. Various available characterization techniques were carried out to investigate and analyze the properties of different electrode materials. Their structural properties were examined using field emission scanning electron microscopy (FESEM), Brunauer-Emmett-Teller (BET), atomic force microscope (AFM), and the elemental analysis was performed using energy dispersive X-ray analysis (EDX). The electrical properties of the nanocomposite samples were characterized using electrochemical impedance spectroscopy (EIS), whereas the capacitance performance was measured by cyclic voltammetry (CV).

MATERIALS AND METHODS
Preparation of Active Materials

Basically, this experimental work is divided into three stages: (i) collecting biomass wastes and producing biochar by slow pyrolysis process, (ii) carbonization process to produce AC, and (iii) mixing with rGO solution for conductive electrode preparation. AC from biochar was prepared through the typical method [7]. Firstly, approximate 20 g of collected dried RSS was mixed with 200 of concentrated solution of KOH in ratio 1:1. After mixing using digital orbital shaker, the mixture was kept for 24h to evaporate the excess water and ensure complete absorption of reagents into the raw materials. Then, the mixture was filtered and washed with distilled water until pH of filtrate was in the range of 6.0 to 7.0. Then, the washed RSS was dried in an oven at 105 for overnight. Next, the second stage of AC production, the carbonization process was carried out. In this process, the dried RSS was placed in a steel crucible and carbonized in a tubular electric furnace under 5 steady flow of N_2 gas at 400 for 3h. The AC derived from RSS (denoted as RSSAC) was cooled to room temperature and washed repeatedly with distilled water to remove the remaining KOH to maintain the pH in the range of 6.0 to 7.0. The RSSAC sample was then dried overnight in an oven at 105. Finally, the bulk RSSAC obtained was pulverized into powder.

The third stage involved synthesis of rGO to be used as an additive in the electrode preparation for a supercapacitor. The detailed preparation procedures are previously described [8]. In this work, two graphite system was applied to obtain GO by applying 5V for 24h. Then, the GO sample was reduced using hydrazine hydrate (80 soluble in water) as a reducing agent with the use of a triple bottle neck. About 1:100 volume ratio of hydrazine hydrate to GO solution was mixed in a container, which was readily immersed in a hot water. The mixture was stirred for 24h using a magnetic stirrer at a temperature ~95. The dispersions were subjected to ultrasonic dissolution for 30 min.

Preparation of Electrodes

In this work, PVA polymer was used as a binder. Prior to the preparation of electrodes, the RSSAC solution was mixed with the PVA at a ratio of 2:8 (denoted as RSSAC/PVA). The mixture was used to coat two nickel plates of dimension of 42.5by spin coating at 1000 for 60s. The samples of RSSAC/PVA were further investigated by adding volumes of rGO, which were denoted as RSSAC/ PVA/rGO. Throughout the experimental work, the ratios of the nanocomposites prepared were

20:79:1, 20:78:2 and 19:78:3, denoted as RSSAC/PVA/rGO$_1$, RSSAC/PVA/rGO$_2$ and RSSAC/PVA/rGO$_3$, respectively.

Characterizations

The samples prepared were subjected to structural, electrical and capacitance investigations. The structural properties were characterized using FEI Nova NanoSEM 450, FESEM equipped with an EDX instrument to identify the elemental composition of the samples. Bruker AXS, Dimension Edge AFM System, was used to investigate the roughness of the prepared samples. All the measurements were carried out at Nano-Optoelectronics Research Centre in School of Physics and School of Chemistry, USM. In addition, the BET surface area measurement was conducted at Surface Morphology Laboratory, School of Chemical Sciences, USM in order to measure RSSAC biochar obtained. Meanwhile, the electrical conductivities of the nanocmposite samples were analyzed using EIS (Gamry Reference 600 Potentiostat/Galvanostat/ZRA), and the capacitance performance was measured using cyclic voltammetry (C-V) (BAS Epsilon version 1.40) instrument.

RESULTS AND DISCUSSION

Fig. 1 (a)-(h) shows the FESEM images of RSSAC/PVA, RSSAC/PVA/rGO$_1$, RSSAC/PVA/rGO$_2$, and RSSAC/PVA/rGO$_3$ samples. Fig. 1 (a)-(b) shows RSSAC with high porosity. The sample revealed that the RSSAC surface is composed of tunnel-shaped pores which were produced during the activation process as depicted in inset of Fig. 1 (b). This might contribute to the greater number of accessible active sites that are beneficial for the ion accumulation and electrochemical double layer formation in charge storage mechanism [9,10]. Meanwhile, Fig. 1 (c)-(d) shows pure rGO exhibiting multilayers and wrinkled sheet-like morphology. The multi-layered rGO was believed to provide a better platform for ion kinetic transportation and improve the performance of the supercapacitor.

Fig. 1 (e) shows the surface morphology of RSSAC/PVA. On addition of PVA in the RSSAC sample, a slightly different morphology was detected. The FESEM image shows that the RSSAC surfaces were covered with PVA polymer and several agglomerated bumpy particles were observed on the surface of PVA. This might be due to the strong interaction between the carbon particles in the RSSAC and PVA polymer, pulling out the carbon particles in RSSAC from the PVA matrix [11]. Moreover, the fabrication of RSSAC/PVA nanocomposite can increase the degradability of charge storage mechanism due to the insulating properties of PVA polymer [12]. Excessive PVA loading may probably decrease the conductivity of the electrodes and it hinders the movement of electrons in the carbon materials. This may inhibit the charge store in the EDL at the RSSAC surface-electrolyte interface, resulting in reduction of the specific capacitance of a supercapacitor [13]. However, the pores of RSSAC were seen to be only partially covered with PVA, thus giving advantages to the ion kinetic movement. Fig. 1 (f)-(h) shows the surface morphology of the various volumes of rGO added into RSSAC/PVA. The FESEM images depicted that rGO has slight effect on the surface morphology of RSSAC/PVA. In several regions, a high degree of agglomerated carbon particles on the smooth surface of PVA was detected. It was observed that excessive PVA generated with increase in volume of rGO. Due to this, conductive carbon particles from rGO start accumulating and covering the RSSAC surface. In general, the EDX spectra of the overall samples reveal that the samples are mainly composed of carbon (C) and oxygen (O). These results have been supported by EDX analysis and are summarized in Table 1.

The EDX analysis confirmed the significant existence peak of carbon (C) and oxygen (O) in the sample. Meanwhile, sodium (Na) and sulphur (S) elements also evolved due to the addition of surfactant during the synthesizing process. Among the electrode samples that used to fabricate the supercapacitor samples, RSSAC/PVA/rGO$_3$ sample has the highest C content of 76.87 wt%, followed by RSSAC/PVA/rGO$_2$ with C content of 74.62 wt%, RSSAC/PVA/rGO$_1$ with C content of 73.07 wt % and RSSAC/PVA with the lowest C content of 71.39 wt %. The C content of the electrode has a positive influence on the capacitance performance of a supercapacitor because the conductive C can maintain the high electrical conductivity of the electrode, improving the capacitance performance of the supercapacitor [14]. However, the capacitance performance starts to decrease as the C content further increases. This is easily acceptable as the excessive conductive C will cover the surface and block the pores in RSSAC and thus affect the effective active sites available for energy
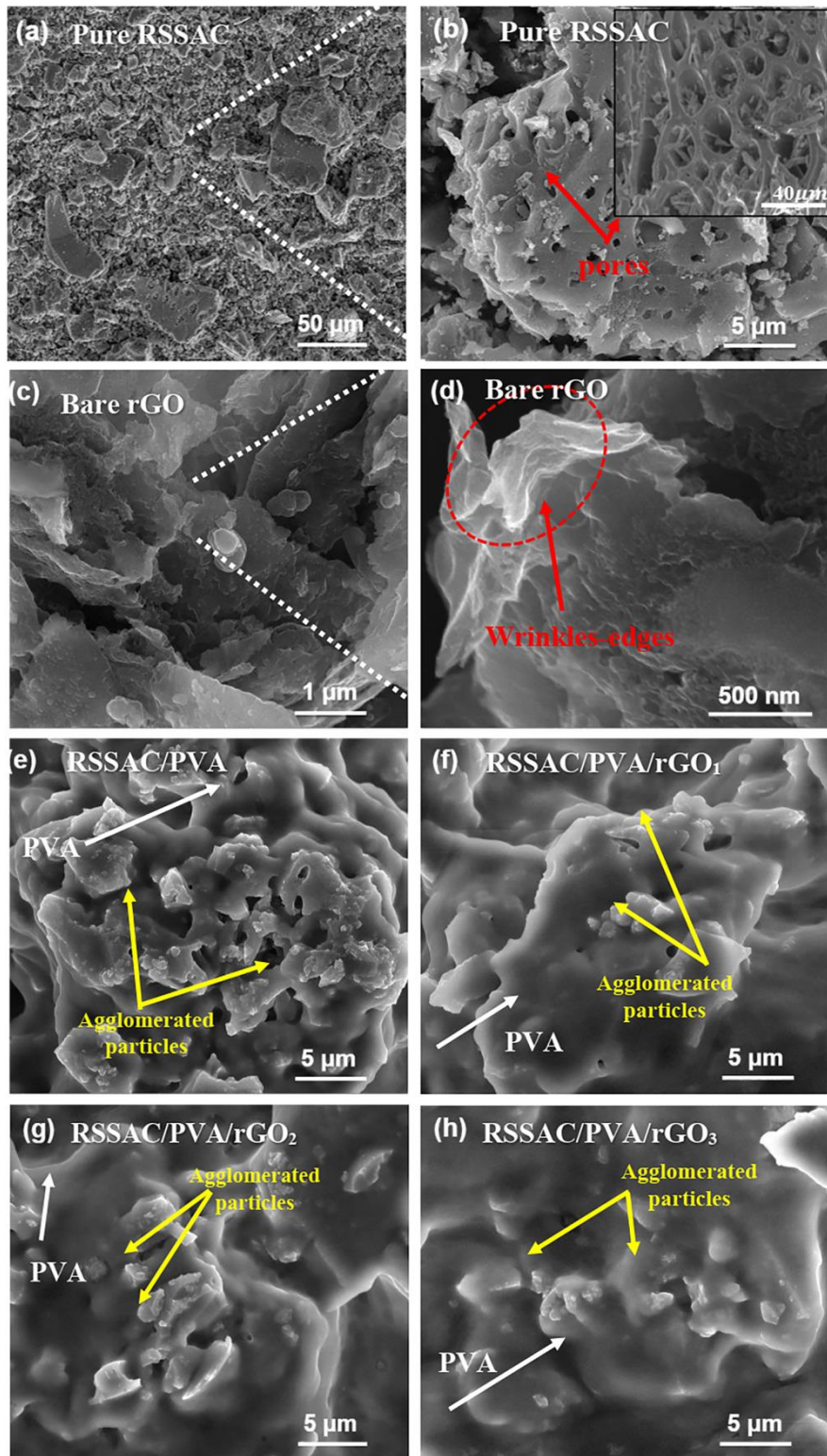
Fig. 1. FESEM images of (a)–(b) pure RSSAC, (c)–(d) bare rGO (e) RSSAC/PVA, (f) RSSAC/PVA/rGO1, (g) RSSAC/PVA/rGO2 and (h) RSSAC/PVA/rGO3 samples.

Table 1. EDX analyses of (a) pure RSSAC, (b) bare rGO, (c) RSSAC/PVA, (d) RSSAC/PVA/rGO1, (e) RSSAC/PVA/rGO2 and (f) RSSAC/PVA/rGO3 samples.

Sample	Element	Atomic %	Weight %
RSSAC	C	91.31	88.73
	O	8.69	11.27
rGO	C	96.98	96.02
	O	3.02	3.98
RSSAC/PVA	C	76.87	71.39
	O	23.13	28.61
RSSAC/PVA/rGO$_1$	C	78.33	73.07
	O	21.67	26.93
RSSAC/PVA/rGO$_2$	C	79.66	74.62
	O	20.34	25.38
RSSAC/PVA/rGO$_3$	C	81.57	76.87
	O	18.43	23.13

storage [15]. This C coating web is intrinsically a physical barrier that hinders the accumulation of opposite charged ions on the surface of electronic conducting electrode that leads to capacity loss [16].

Fig. 3 shows AFM images of the samples, and the results are summarized in Table 2. There was decrease in roughness after addition a small portion of rGO is added into RSSAC/PVA sample. However, when the volume of rGO increased, the roughness also increased until it reached another high value on RSSAC/PVA/rGO$_3$ sample. The results obtained were supported by FESEM image (Fig. 1). The roughness of RSSAC/PVA sample was contributed by its SSA due to the agglomeration of C element on the PVA surface and the pores that the pores that were not covered by PVA. Since a small volume of rGO was injected into the samples, the roughness was decreased with the SSA because some pores in RSSAC were filled by rGO. The more the rGO added, the more the excessive PVA and more C particles of rGO accumulated on the RSSAC surface, then increasing its roughness.

Basically, the roughness was closely related to the SSA and the pore volume of the RSSAC. Therefore, in order to further confirm the relationship between the SSA of the RSSAC

sample with the roughness of nanocomposites produced, the nitrogen adsorption isotherm was carried out as shown in Fig. 3 (e). From these nitrogen adsorption isotherm spectra, the SSA and the pore volume were measured to be 1.78 and 2.7, respectively. A significant increase in nitrogen uptake at low pressure was detected and further increase was noted with respect to pressure. Moreover, a small and narrow hysteresis loop observed at two regions of range 0.0-0.5 and 0.5-1.0 further confirmed the existence of micropore and mesopore volume, respectively, within the carbon structures [17, 18]. Various kinds of pore distributions were beneficial for the ion penetration and adsorption during charge discharge as they provide a better platform for increasing the interaction between RSSAC and rGO sheets.

Numerous studies attempted to determine the relationship between surface roughness and capacitance performance, and some researchers found that the performance of a supercapacitor increases with the surface roughness [19,20]. However, because the roughness of the samples is mainly contributed by the accumulation and agglomeration of PVA and rGO on RSSAC, so the properties and effect of PVA and rGO to
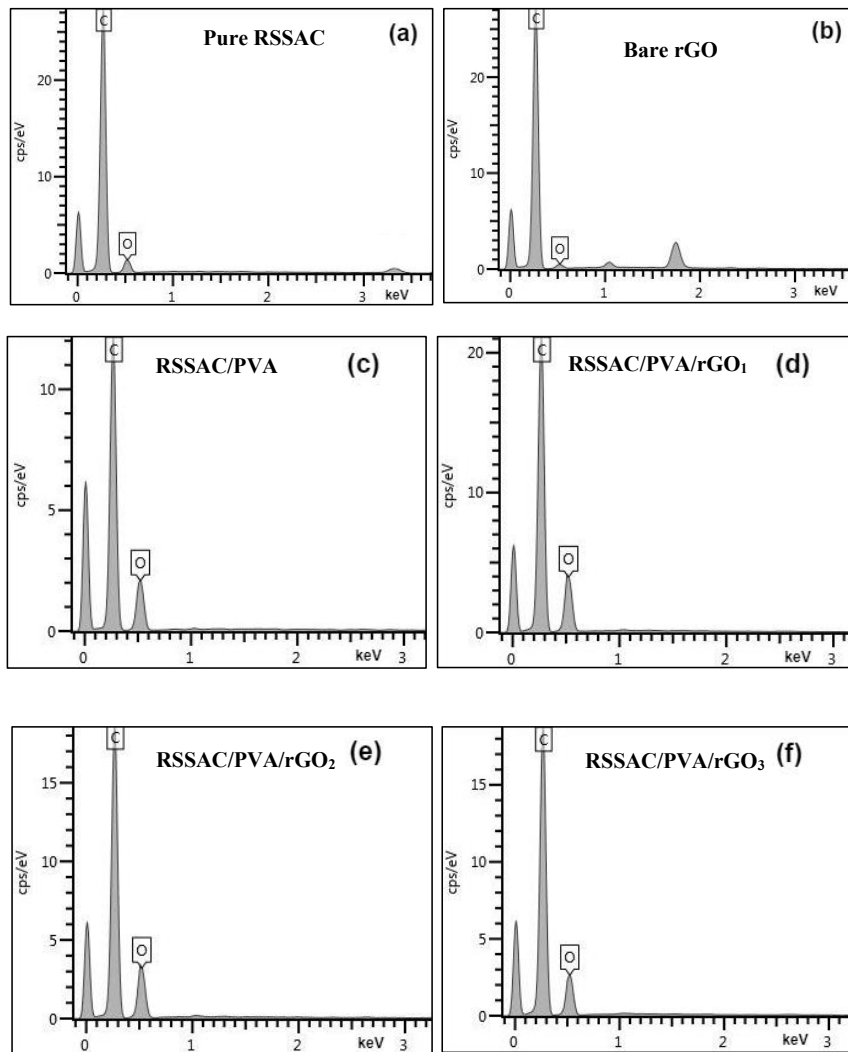
Fig. 2. EDX analyses of (a) pure RSSAC, (b) bare rGO, (c) RSSAC/PVA, (d) RSSAC/PVA/rGO1, (e) RS-SAC/PVA/rGO2 and (f) RSSAC/PVA/rGO3 samples.

the capacitance performance should be taken into consideration primarily in this study. It was observed that the mixing of RSSAC with PVA significantly degrade the high potential of charge storage in the sample. The PVA polymer has blocked the pore size of RSSAC and subsequently decreased the SSA of RSSAC, which then limited the propagation of the ion diffusion. Hence, the introduction of rGO in the RSSAC/PVA sample was believed to improve the capacitance performance by providing a platform for ion diffusion between the interlayer spacing sheets. The existence of the oxygen functional group in rGO surfaces such as epoxy, carboxyl, carbonyl and hydroxyl functional group can improve the wettability in aqueous systems by altering surface effects [10]. Due to good wettability performed by rGO sheets, it contributed to better accessibility for ions in the electrolyte to form EDL at the interface with the RSSAC surface, thus achieving higher capacitance [10,21].

Fig. 4 shows the Nyquist plots for all composite samples. From the results, the semi-circles seen indicate the process of transferring charges of the electrolyte ions onto the RSSAC surface. From the Nyquist plots, the diameter of the semicircle represents the interfacial charge transfer of resistance which can be calculated by the difference between two end points of a semicircle on the -axis. A decrease in diameter of semicircle
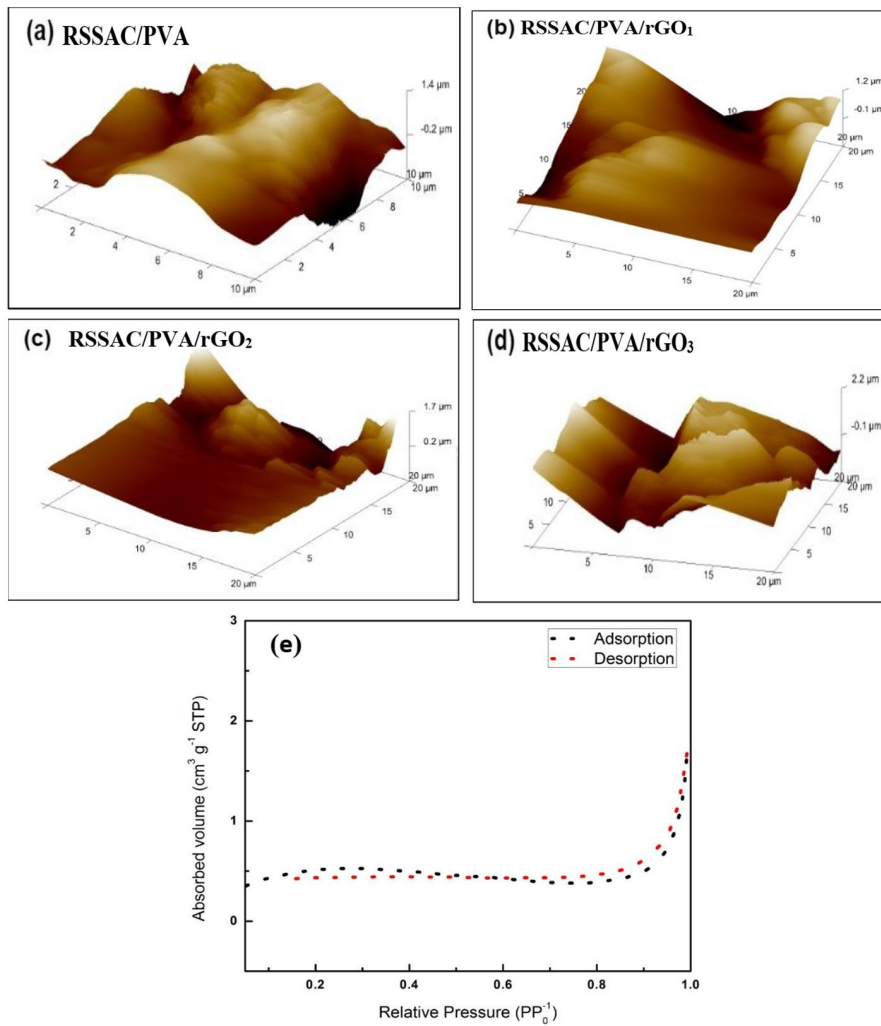
Fig. 3. AFM images of (a) RSSAC/PVA, (b) RSSAC/PVA/rGO1, (c) RSSAC/PVA/rGO2 and (d) RSSAC/PVA/rGO3 samples and (e) Nitrogen adsorption-desorption isotherm of BET analysis.

Table 2. The roughness parameters (Ra and Rq) of RSSAC/PVA, RSSAC/PVA/rGO1, RSSAC/PVA/rGO2, RSSAC/PVA/rGO3 samples.

Sample	Roughness Parameters	
	Root mean square roughness, R_q (μm)	Average roughness, R_a (μm)
RSSAC/PVA	0.459	0.381
RSSAC/PVA/rGO$_1$	0.398	0.342
RSSAC/PVA/rGO$_2$	0.483	0.361
RSSAC/PVA/rGO$_3$	0.484	0.364
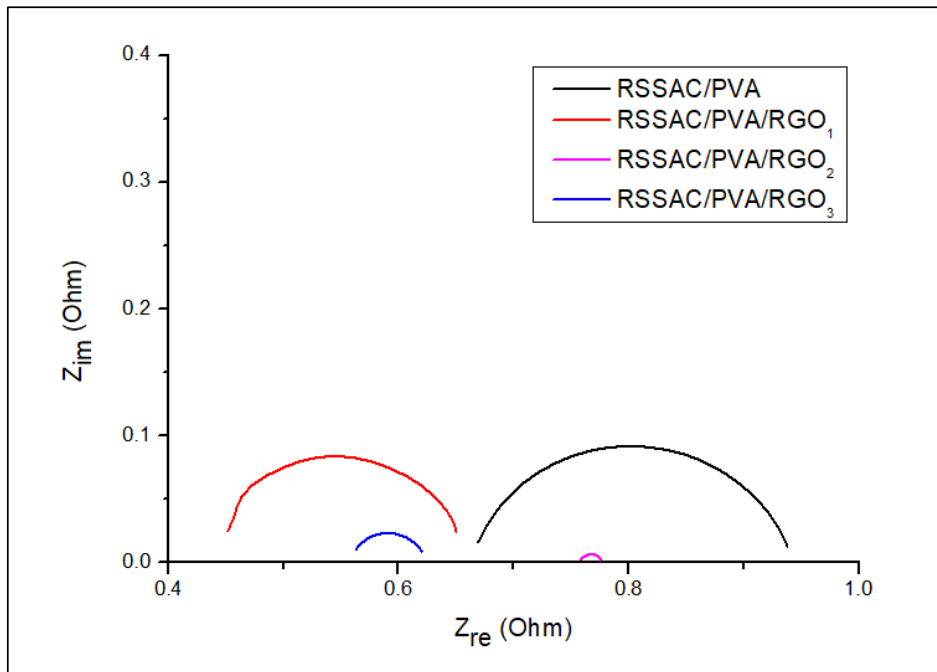
Fig. 4.   Nyquist impedance plots for RSSAC/PVA, RSSAC/PVA/rGO1, RSSAC/PVA/rGO2 and RSSAC/PVA/ rGO3 samples.

Table 3. The resistance, resistivity and conductivity of RSSAC/PVA, RSSAC/PVA/rGO1, RSSAC/PVA/rGO2, RSSAC/ PVA/rGO3 samples.

Sample	Resistance, R (mΩ)	Resistivity, ρ (Ω.cm)	Conductivity, σ (S/cm)
RSSAC/PVA	278.3	71.36	0.0140
RSSAC/PVA/rGO$_1$	220.2	56.46	0.0177
RSSAC/PVA/rGO$_2$	14.58	3.738	0.2675
RSSAC/PVA/rGO$_3$	62.32	15.98	0.0626

means a decrease of resistance or an increase of conductivity that renders the increase of specific capacitance values [22]. A supercapacitor that is made up of active materials of high SSA and electrodes of low resistance has overcome the ability to form electric charges [23]. The numerical data is presented in Table 3.

The resistance values for each sample can be obtained directly from the EIS system. The results showed that the RSSAC/PVA/rGO$_2$ sample has the highest conductivity of 0.2675 S/cm, followed by the RSSAC/PVA/rGO$_3$ sample with a conductivity of 0.0626 S/cm, and the RSSAC/PVA/rGO$_1$ sample

with a conductivity of 0.0177 S/cm. The RSSAC/ PVA sample has the lowest conductivity with a value of 0.0140 S/cm. The increasing pattern of conductivity in the RSSAC/PVA/rGO$_2$ samples is due to the presence of sufficient amount of C in rGO surfaces. These conductive C improved the electrical conductivity of the electrode. In addition, the oxygen functional groups that existed in the rGO surfaces also increase the conductivity by improving the wettability in aqueous systems, hence increasing the capacitance performance. However, the excessive amount of 3 wt% rGO in the sample was believed to create a C coating
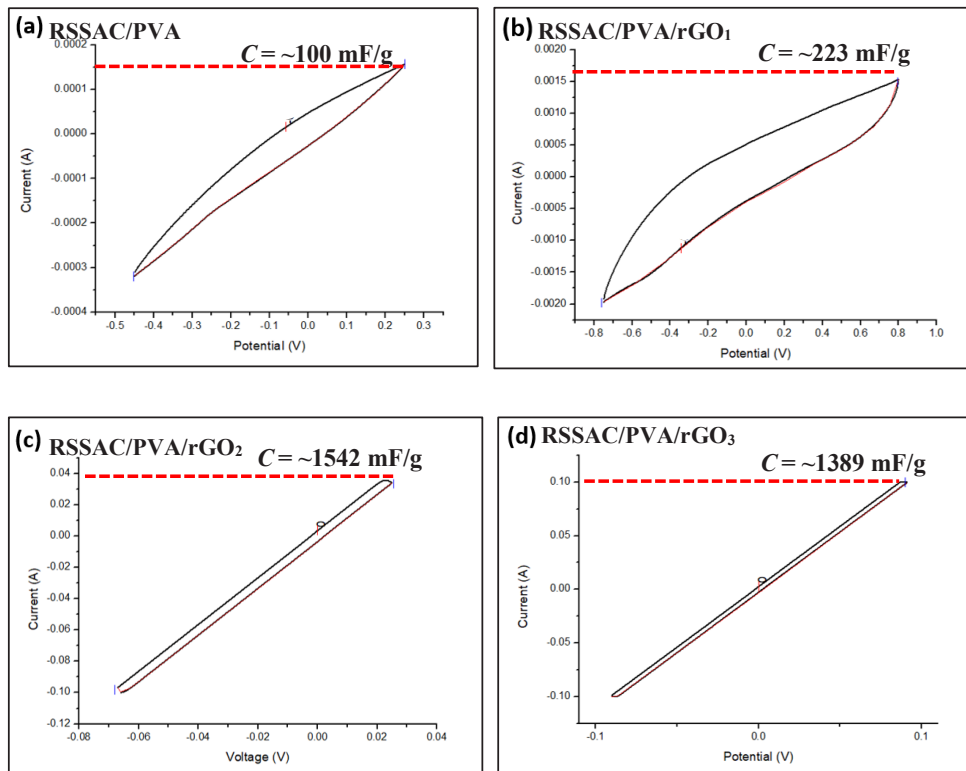
Fig. 5. Cyclic voltammetry of (a) RSSAC/PVA, (b) RSSAC/PVA/rGO1, (c) RSSAC/PVA/rGO2 and (d) RSSAC/PVA/rGO3 samples.

web, which acts as a physical barrier that covers the conductive surface and inhibits the accumulation of the electrolyte ions onto the pores of the opposite charged electrode. This led to the decrease in conductivity of the RSSAC/PVA/rGO$_3$ sample. This trend can also be explained by the presence of insulated PVA and conductive C in rGO. The excessive PVA content has reduced the conductivity of the supercapacitor electrode, thereby reducing the capacitance performance of the supercapacitors [22,23]. However, the insufficient PVA content also led to an adhesion issue [21]. Therefore, the rGO and PVA content play a role in obtaining the best synergetic effect and configuration of electrode materials for supercapacitor application.

CV was carried out to characterize the capacitive behavior of a supercapacitor as shown in Fig. 5. From the results, the RSSAC/PVA/rGO$_2$ sample showed the highest specific capacitance of up to 1542.7 mF/g, followed by the RSSAC/PVA/rGO$_3$ with a specific capacitance of 1388.7 mF/g, and the RSSAC/PVA/rGO$_1$ sample with a specific capacitance of 223.0 mF/g. The RSSAC/PVA sample

has the lowest value of specific capacitance of 104.0 mF/g. The results were consistent with the EIS results. RSSAC/PVA sample showed the lowest conductivity (0.0140 S/cm) and the lowest specific capacitance (104 mF/g). This was due to the characteristics of a high PVA content in its electrodes. The surface and the pores of RSSAC have been covered by PVA, and this restricted the movement of ions within the electrodes. In addition, the insulating properties of PVA also degraded the conductivity of the sample and limited the diffusion of ions into the pores of RSSAC. Moreover, RSSAC/PVA sample has the lowest C content among the other samples, which contributed to the lowest conductive network.

As compared to the composite samples with presence of rGO sheets, the conductivity and the specific capacitance was suddenly increased. This was due to the presence of rGO that increases the conductive network in the samples, thus improving its conductivity and specific capacitance. Moreover, the oxygen functional groups in rGO have improved the wettability of the sample, which offers a better pathway of ions to access in

Table 4. The parameters used and the specific capacitances of RSSAC/PVA, RSSAC/PVA/rGO1, RSSAC/PVA/rGO2, RSSAC/PVA/rGO3 samples.

Sample	s (mV/s)	m (g)	ΔV (V)	$\int I\, dV$ (x10⁻⁴)	C_S (F/g)
RSSAC/PVA		0.0252	0.7	0.1850	0.0104
RSSAC/PVA/rGO₁		0.0201	1.55	6.9461	0.2230
RSSAC/PVA/rGO₂	100	0.0220	0.092	3.1224	1.5427
RSSAC/PVA/rGO₃		0.0204	0.18	5.0993	1.3887

the small pores of RSSAC. It can clearly be seen that the increase in specific capacitance is reflected by increasing the amount of rGO in the composite sample. The presence of higher amount of rGO increases the sample roughness because of excess PVA and rGO that had accumulated on the surface of RSSAC. It also increases the conductive C content to steeply improve the electrical conductivity from 0.0177 S/cm in RSSAC/PVA/rGO₁ sample to 0.2675 S/cm in RSSAC/PVA/rGO₂ sample, and the specific capacitance from 223 mF/g to 1542.7 mF/g. The sample with 2 wt% of rGO has the best capacitance performance as compared to the other samples with 0 wt%, 1 wt%, and 3 wt% of rGO present in the composite RSSAC/PVA.

However, the specific capacitance was reduced to 1388.7 mF/g for the RSSAC/PVA/rGO₃ sample because the excessive PVA and conductive C have blocked the pores in RSSAC, thus reducing the effectiveness of active sites for kinetic ion movement to transfer the charges between the electrodes. The excessive C coating web was believed to be an intrinsically physical barrier that hinders the diffusion and accumulation of ions on the RSSAC surface, resulting in capacity loss. This dramatically cause the decrease in electrical conductivity of the sample from 0.2675 S/cm to 0.0626 S/cm. Details on capacitive behavior have been summarized in Table 4.

CONCLUSION

The results show that the sufficient volume of rGO contributed to the capacitance performance since the C content and roughness increased with rGO. Among other samples, the RSSAC/PVA/rGO₂ supercapacitor sample showed the best electrochemical behaviour. The highest electrical conductivity (0.2675 S/cm) and

specific capacitance value (1542.7 mF/g) were obtained from the sample. This was due to the presence of an appropriate amount of rGO that enhanced the electrochemical performance of the supercapacitor. The conductive C inside the rGO increased the conductivity of the electrode. Moreover, the oxygen functional groups improved the wettability in aqueous system and hence increased the specific capacitance of the supercapacitor. Therefore, the spread of a small amount of rGO in enhancing the capacitive behavior has potentially showed its ability to be implemented as a conductive electrode material in supercapacitor applications.

ACKNOWLEDGEMENT

CONFLICT OF INTEREST

The authors declare that there is no conflict of interests regarding the publication of this manuscript.

REFERENCES

1. Gunawardane K. Capacitors as energy storage devices—simple basics to current commercial families. Energy Storage Devices for Electronic Systems: Elsevier; 2015. p. 137-148.
2. Sartova K, Omurzak E, Kambarova G, Dzhumaev I, Borkoev B, Abdullaeva Z. Activated carbon obtained from the cotton processing wastes. Diamond Relat Mater. 2019;91:90-97.
3. Zhang J, Tahmasebi A, Omoriyekomwan JE, Yu J. Production of carbon nanotubes on bio-char at low temperature via microwave-assisted CVD using Ni catalyst. Diamond Relat Mater. 2019;91:98-106.

4. S. Iro Z. A Brief Review on Electrode Materials for Supercapacitor. International Journal of Electrochemical Science. 2016:10628-10643.

5. Lota K, Sierczynska A, Acznik I, Lota G. Effect of aqueous electrolytes on electrochemical capacitor capacitance. Chemik. 2013;67(11):1138-1145.

6. Joshi S, Pokharel BP. Preparation and Characterization of Activated Carbon from Lapsi (Choerospondias axillaris) Seed Stone by Chemical Activation with Potassium Hydroxide. Journal of the Institute of Engineering. 2014;9(1):79-88.

7. Md Disa N, Abu Bakar S, Alfarisa S, Mohamed A, Md Isa I, Kamari A, et al. The Synthesis of Graphene Oxide via Electrochemical Exfoliation Method. Advanced Materials Research. 2015;1109:55-59.

8. Misnon II, Zain NKM, Aziz RA, Vidyadharan B, Jose R. Electrochemical properties of carbon from oil palm kernel shell for high performance supercapacitors. Electrochim Acta. 2015;174:78-86.

9. Yu A, Chabot V, Zhang J. Electrochemical supercapacitors for energy storage and delivery: fundamentals and applications. CRC press; 2017 Dec 19.

10. Zhou X-W, Zhu Y-F, Liang J. Preparation and properties of powder styrene–butadiene rubber composites filled with carbon black and carbon nanotubes. Mater Res Bull. 2007;42(3):456-464.

11. Nur Fazreen A, Hanafi I, Mohamad Kahar Ab W, Santiagoo R, Hosta A, Sam Sung T. Development of New Material Based on Polyvinyl Alcohol/Palm Kernel Shell Powder Biocomposites. Advances in Environmental Studies. 2018;2(2).

12. Tsay K-C, Zhang L, Zhang J. Effects of electrode layer composition/thickness and electrolyte concentration on both specific capacitance and energy density of supercapacitor. Electrochim Acta. 2012;60:428-436.

13. Park S, Kim S. Effect of carbon blacks filler addition on electrochemical behaviors of Co_3O_4/graphene nanosheets as a supercapacitor electrodes. Electrochim Acta. 2013;89:516-522.

14. Ranade AP. Optimization study of supercapacitor electrode material and thickness for its enhanced performance. State University of New York at Binghamton; 2011.

15. Zhou N, Uchaker E, Liu YY, Liu SQ, Liu YN, Cao GZ. Effect of carbon content on electrochemical performance of $LiFePO_4$/C thin film cathodes. Int. J. Electrochem. Sci. 2012 Dec 1;7:12633-12645.

16. Zhang HF, Liu XW, Li H, Chen N, Fu YB. Effect of the Surface Roughness on the Detecting Capacitance. Key Eng Mater. 2013;562-565:1461-1466.

17. Sanchez-Sanchez A, Izquierdo MT, Mathieu S, González-Álvarez J, Celzard A, Fierro V. Outstanding electrochemical performance of highly N- and O-doped carbons derived from pine tannin. Green Chem. 2017;19(11):2653-2665.

18. Zhang J. Nitrogen-rich Porous Carbon Derived from Biomass as High Performance Electrode Materials for Supercapacitors. International Journal of Electrochemical Science. 2018:5204-5218.

19. Albina A, Taberna PL, Cambronne JP, Simon P, Flahaut E, Lebey T. Impact of the surface roughness on the electrical capacitance. Microelectron J. 2006;37(8):752-758.

20. Gao Y. Graphene and Polymer Composites for Supercapacitor Applications: a Review. Nanoscale Research Letters. 2017;12(1).

21. Chen SM, Ramachandran R, Mani V, Saraswathi R. Recent advancements in electrode materials for the high-performance electrochemical supercapacitors: a review. Int. J. Electrochem. Sci. 2014 Aug 1;9(8):4072-4085.

22. Mohapatra S, Acharya A, Roy GS. The role of nanomaterial for the design of supercapacitor. Lat. Am. J. Phys. Educ. Vol. 2012 Sep;6(3):380.

23. Suriani AB, Nurhafizah MD, Mohamed A, Masrom AK, Sahajwalla V, Joshi RK. Highly conductive electrodes of graphene oxide/natural rubber latex-based electrodes by using a hyper-branched surfactant. Materials & Design. 2016;99:174-181.